living planet symposium | BONN 23–27 May 2022

TAKING THE PULSE OF OUR PLANET FROM SPACE

EUMETSAT ECMWF EUSPA

Toward fair validation of AI algorithms for (not only) EO

Jakub Nalepa | jnalepa@ieee.org | KP Labs/Silesian University of Technology

KP LABS

May 27, 2022

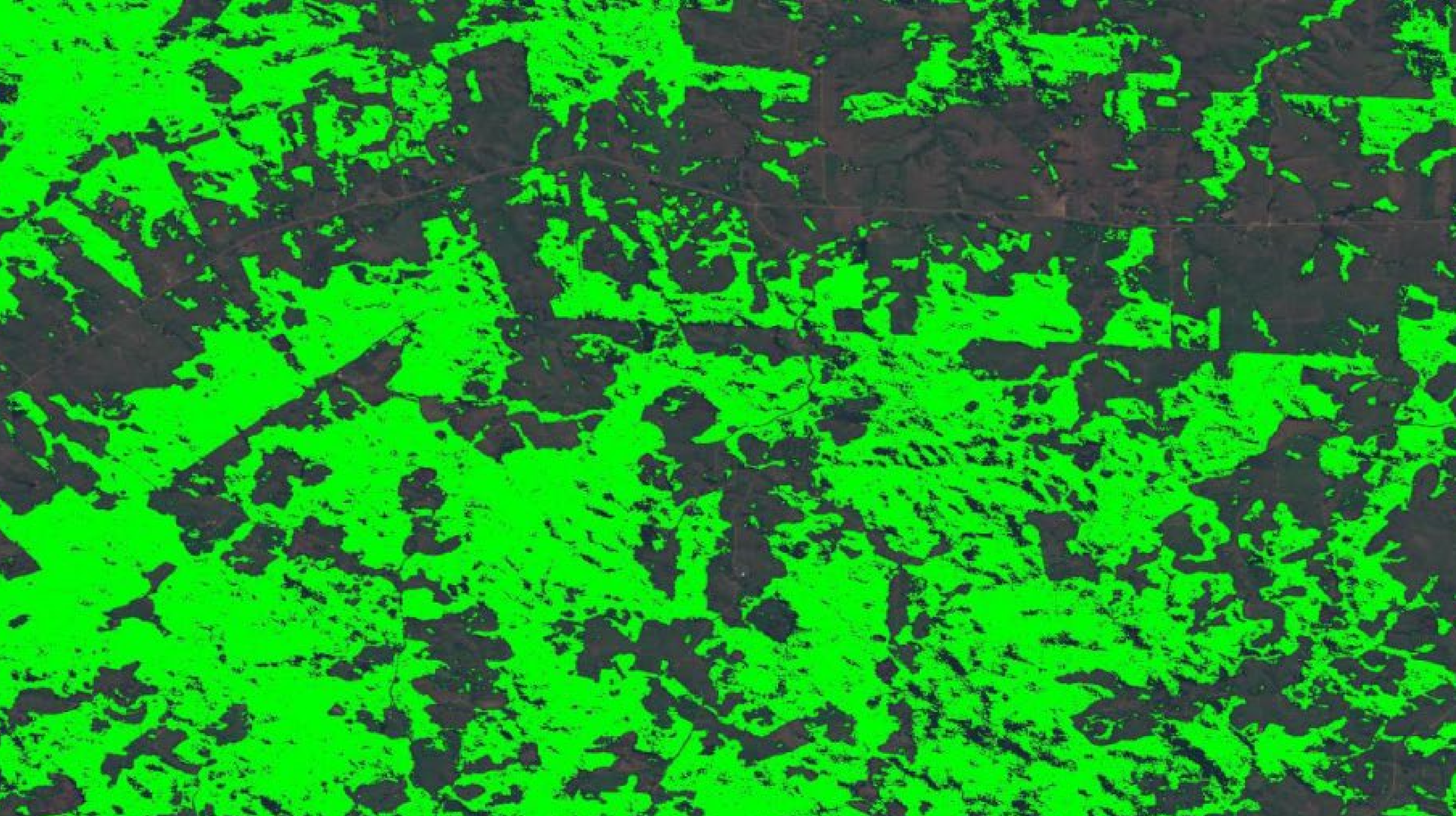

Toward high-quality training sets

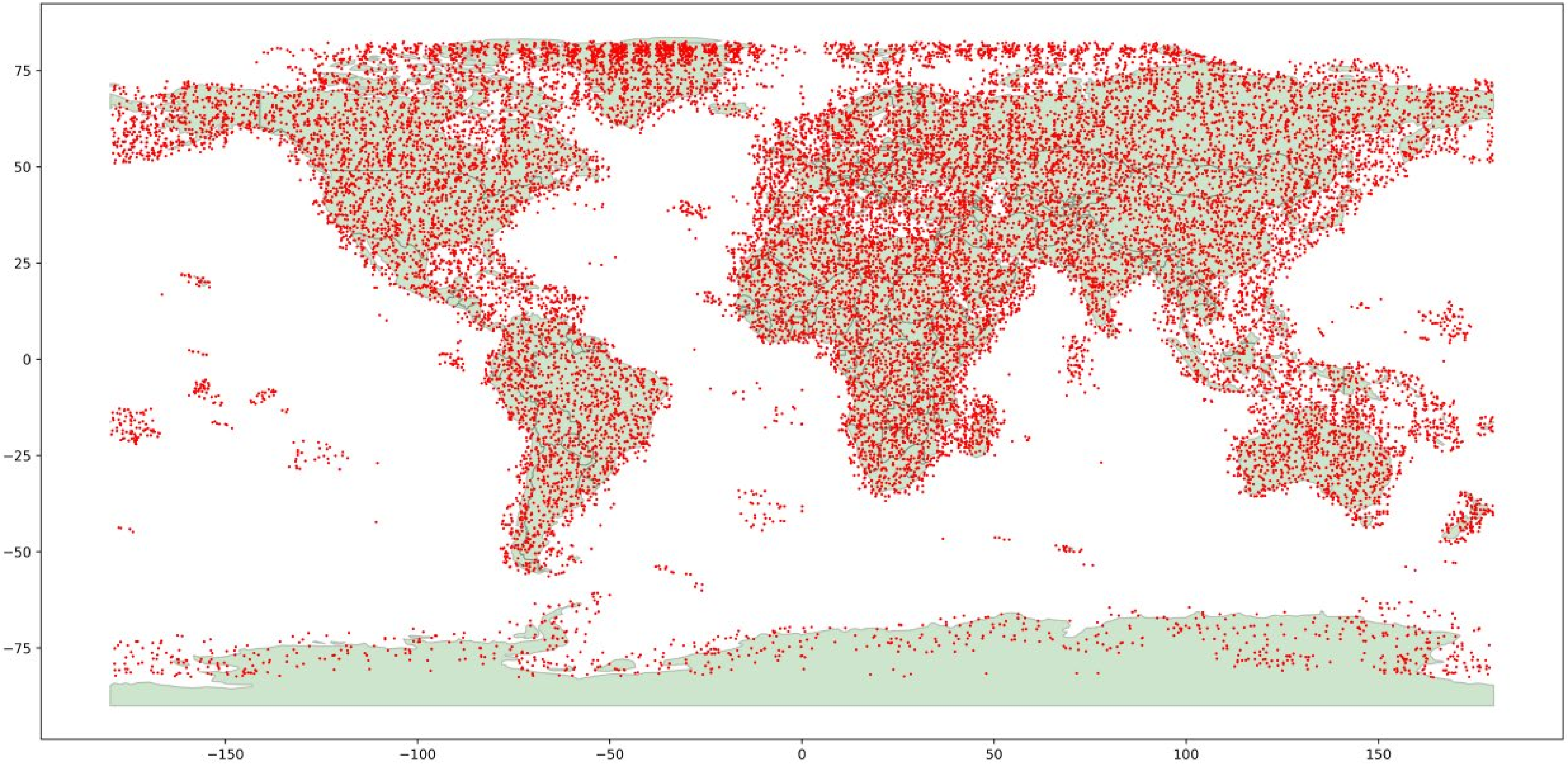

J. Giuffrida, et al.: The Φ-Sat-1 Mission: The First On-Board Deep Neural Network Demonstrator for Satellite Earth Observation, IEEE TGRS, 2021, DOI: 10.1109/TGRS.2021.3125567.

Training-test information leak

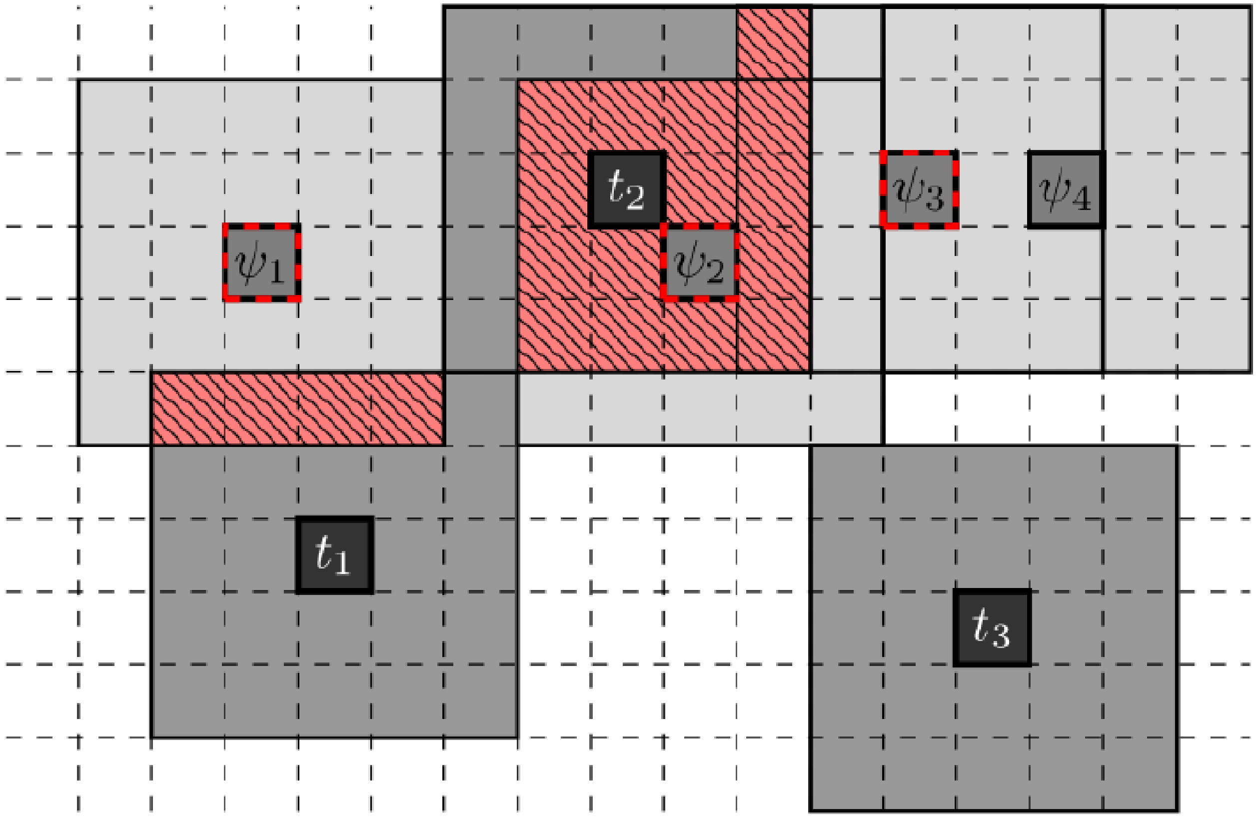

J. Nalepa, M. Myller, M. Kawulok: Validating Hyperspectral Image Segmentation. IEEE Geosci. Remote. Sens. Lett. 16(8): 1264-1268 (2019)

Training-test information leak

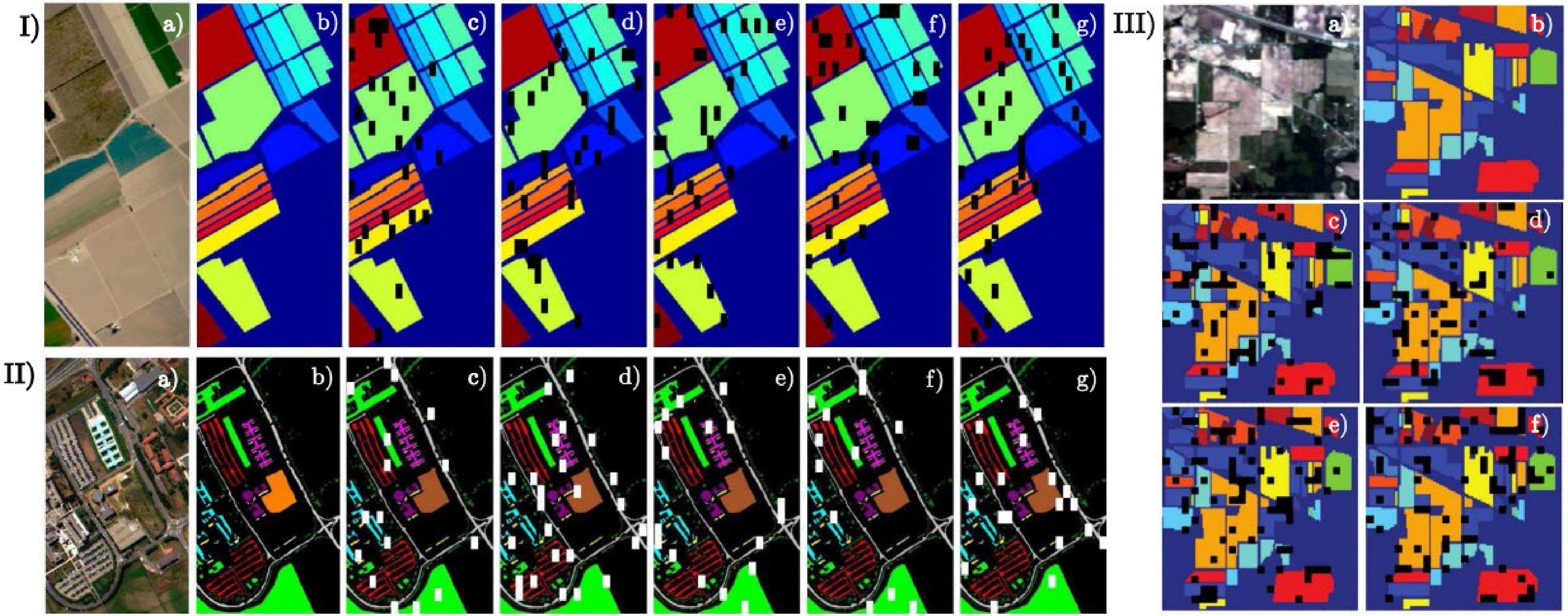

Our benchmark data generated over the (I) Salinas Valley (five nonoverlapping folds), (II) Pavia University (five folds), and (III) Indian Pines (four folds) sets. (a) True color composite. (b) Ground truth. (c)–(g) Visualization of all folds for Salinas and Pavia. (c)–(f) For Indian Pines: black (white for Pavia University) patches contain training pixels, whereas the other pixels are taken as test data.

J. Nalepa, M. Myller, M. Kawulok: Validating Hyperspectral Image Segmentation. IEEE Geosci. Remote. Sens. Lett. 16(8): 1264-1268 (2019)

Training-test information leak

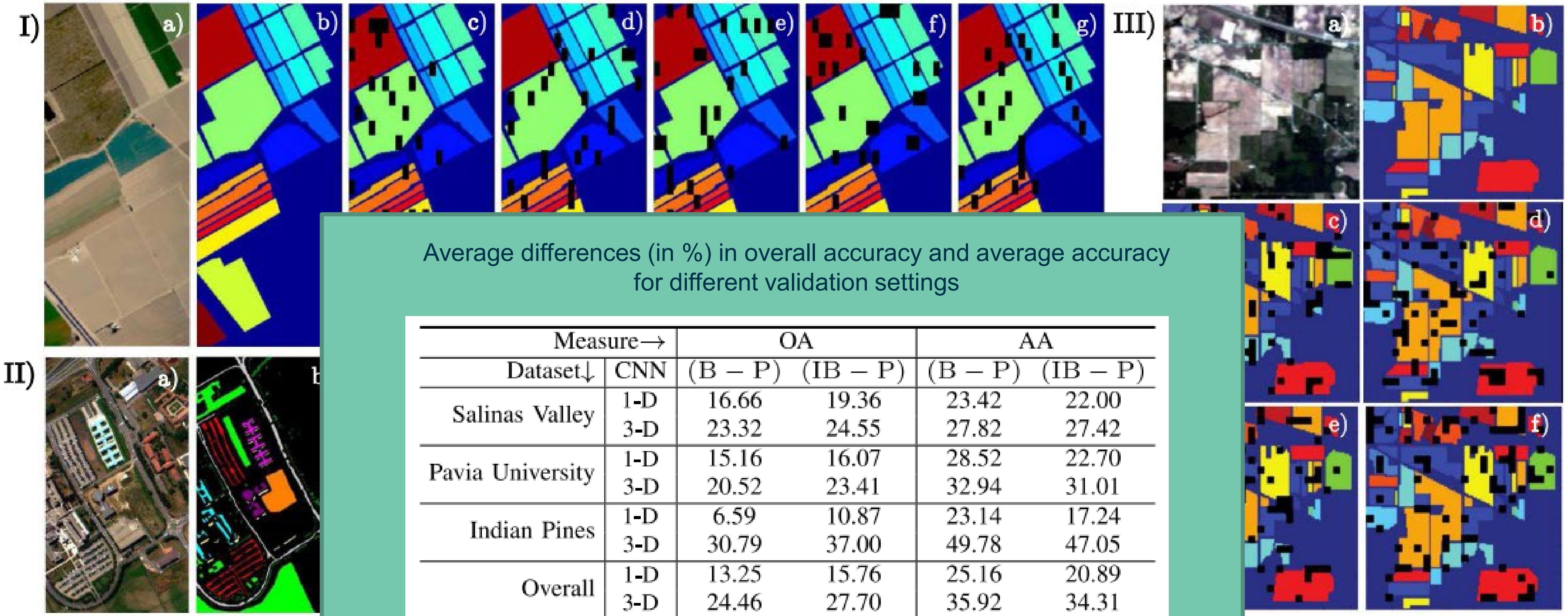

Average differences (in %) in overall accuracy and average accuracy for different validation settings

Measure→		OA		AA	
Dataset↓	CNN	(B – P)	(IB – P)	(B – P)	(IB – P)
Salinas Valley	1-D	16.66	19.36	23.42	22.00
	3-D	23.32	24.55	27.82	27.42
Pavia University	1-D	15.16	16.07	28.52	22.70
	3-D	20.52	23.41	32.94	31.01
Indian Pines	1-D	6.59	10.87	23.14	17.24
	3-D	30.79	37.00	49.78	47.05
Overall	1-D	13.25	15.76	25.16	20.89
	3-D	24.46	27.70	35.92	34.31

Our benchmark data generated over th II) Indian Pines (four folds) sets. (a) True color composite. (b) Ground truth. (c)–(g) Visualization of all folds for Salinas and Pavia. (c)–(f) For Indian Pines: black (white for Pavia University) patches contain training pixels, whereas the other pixels are taken as test data.

J. Nalepa, M. Myller, M. Kawulok: Validating Hyperspectral Image Segmentation. IEEE Geosci. Remote. Sens. Lett. 16(8): 1264-1268 (2019)

Toward on-board processing: data-level digital twin

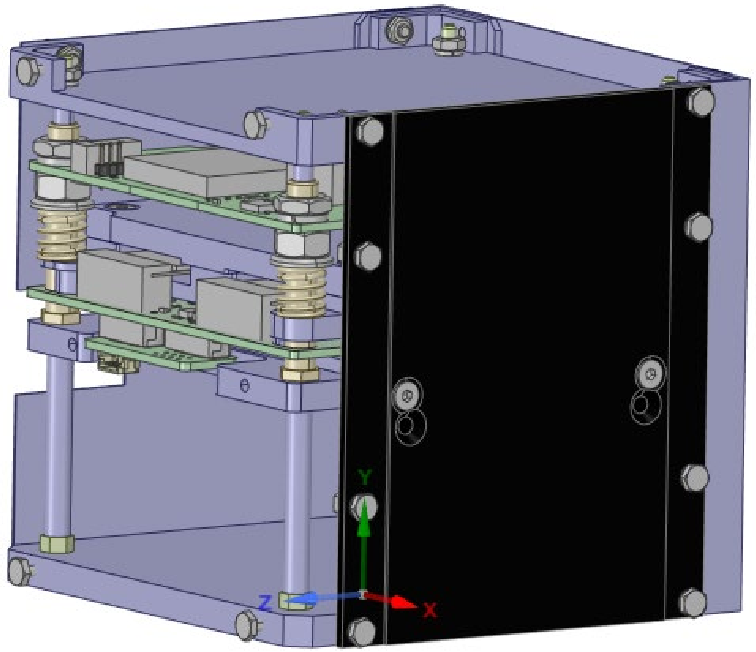

Toward on-board processing: data-level digital twin

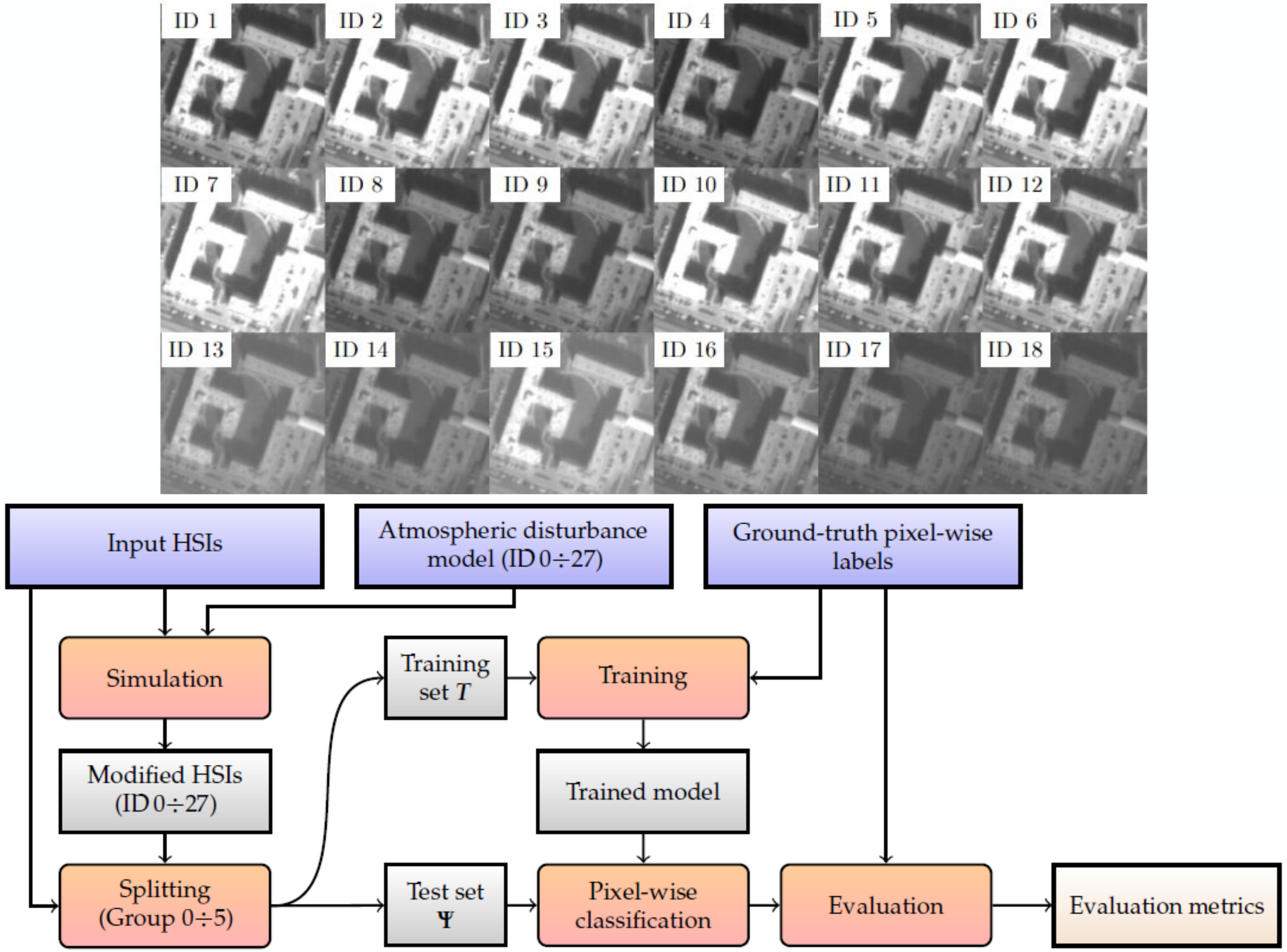

J. Nalepa et al.: Towards on-board hyperspectral satellite segmentation, Remote Sensing 2021, 13(8), 1532 (https://www.mdpi.com/2072-4292/13/8/1532)

Toward on-board processing: data-level digital twin

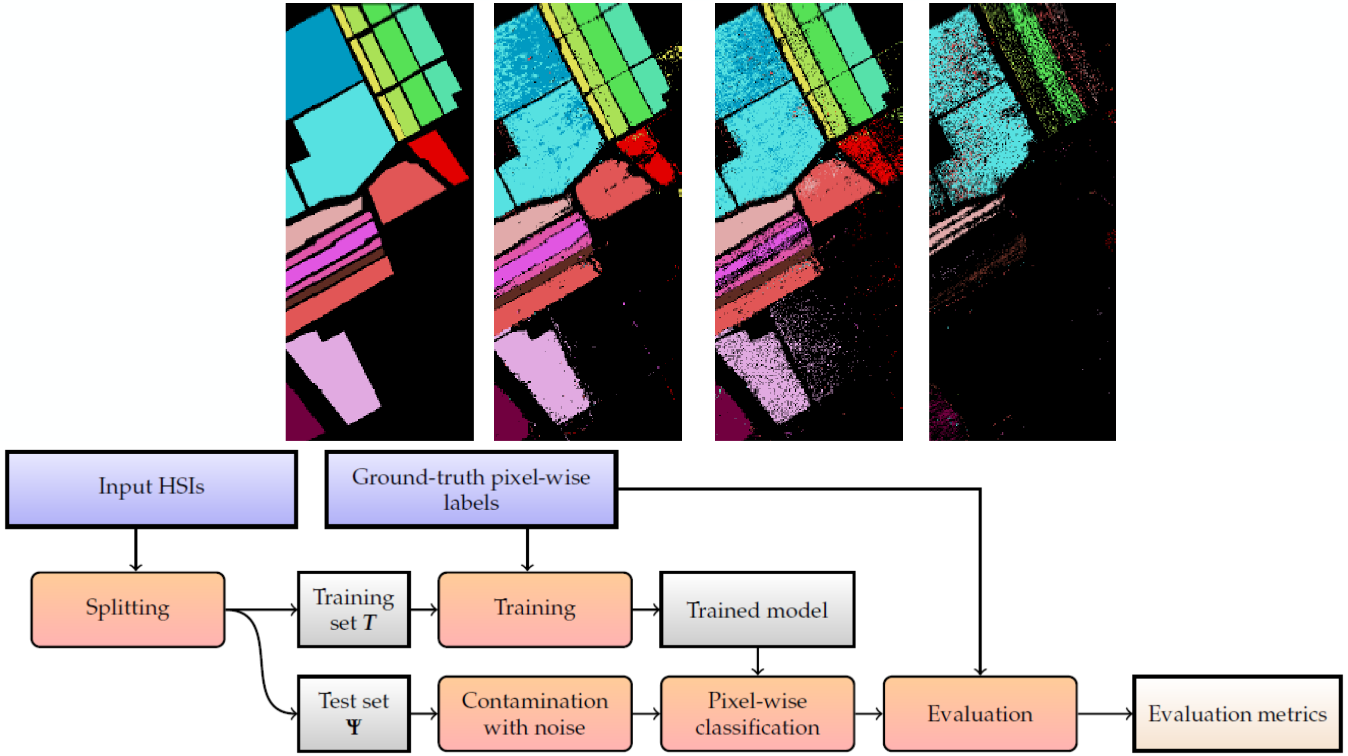

J. Nalepa et al.: Towards on-board hyperspectral satellite segmentation, Remote Sensing 2021, 13(8), 1532 (https://www.mdpi.com/2072-4292/13/8/1532)

Toward on-board processing: data-level digital twin

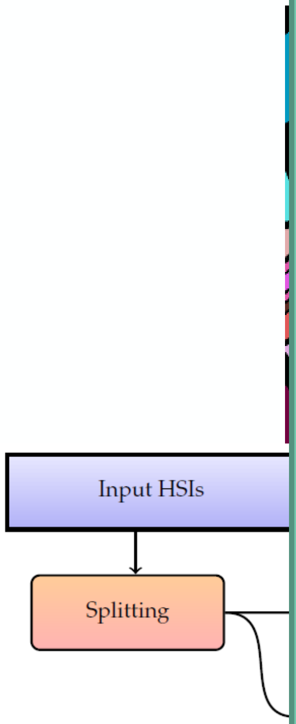

Example: Differences between metrics for uncontaminated and noisy HSI in hyperspectral classification (average over four benchmarks, Indian Pines, Salinas Valley, Pavia University and Houston)

1D CNN

	Gaussian					Impulsive					Poisson				
$\eta_P \rightarrow$	0.1	0.2	0.3	0.4	0.5	0.1	0.2	0.3	0.4	0.5	0.1	0.2	0.3	0.4	0.5
OA	0.87	1.74	2.61	3.50	4.35	5.15	10.28	15.41	20.62	25.76	4.16	8.33	12.51	16.61	20.83
BA	0.98	1.92	2.77	3.76	4.67	4.91	9.72	14.68	19.47	24.36	3.99	8.04	12.13	16.07	20.12
κ	1.12	2.23	3.34	4.48	5.58	6.03	11.95	17.87	23.66	29.46	4.97	9.94	14.91	19.76	24.74
OA′	−0.35	0.54	1.43	2.34	3.22	4.16	9.56	15.00	20.43	25.83	3.14	7.54	11.96	16.28	20.74
BA′	−0.60	0.53	1.54	2.73	3.81	4.15	9.97	15.91	21.71	27.63	2.96	7.76	12.62	17.29	22.10
κ'	−0.71	0.44	1.59	2.77	3.92	4.92	11.51	18.03	24.52	30.88	3.51	8.87	14.22	19.44	24.79

2.5D CNN

	Gaussian					Impulsive					Poisson				
$\eta_P \rightarrow$	0.1	0.2	0.3	0.4	0.5	0.1	0.2	0.3	0.4	0.5	0.1	0.2	0.3	0.4	0.5
OA	0.08	0.09	0.09	0.10	0.12	4.53	8.97	13.43	17.90	22.32	1.58	3.09	4.57	6.09	7.59
BA	0.13	0.15	0.15	0.16	0.20	4.05	7.98	11.87	15.78	19.68	1.61	3.08	4.54	6.01	7.50
κ	0.10	0.12	0.13	0.14	0.17	5.03	9.88	14.69	19.43	24.15	2.04	4.01	5.98	7.99	10.00
OA′	0.08	0.09	0.09	0.11	0.12	4.83	9.55	14.32	19.07	23.84	1.62	3.17	4.70	6.26	7.80
BA′	0.16	0.18	0.18	0.20	0.23	4.88	9.61	14.25	18.94	23.69	1.93	3.70	5.46	7.23	9.02
κ'	0.10	0.12	0.13	0.15	0.17	5.87	11.57	17.17	22.68	28.13	2.11	4.15	6.18	8.26	10.35

3D CNN

	Gaussian					Impulsive					Poisson				
$\eta_P \rightarrow$	0.1	0.2	0.3	0.4	0.5	0.1	0.2	0.3	0.4	0.5	0.1	0.2	0.3	0.4	0.5
OA	0.07	0.12	0.18	0.24	0.30	3.90	7.74	11.61	15.46	19.33	3.07	6.11	9.17	12.22	15.22
BA	−0.04	0.02	0.09	0.15	0.21	4.16	8.43	12.65	16.92	21.19	3.21	6.54	9.85	13.17	16.45
κ	0.03	0.10	0.17	0.25	0.32	5.00	10.01	15.04	20.07	25.22	3.82	7.66	11.55	15.43	19.29
OA′	0.07	0.13	0.19	0.25	0.74	4.06	8.09	12.12	16.14	20.18	3.25	6.47	9.71	12.94	16.12
BA′	−0.05	0.03	0.10	0.16	−0.19	4.96	10.06	15.06	20.16	25.26	3.78	7.70	11.60	15.50	19.37
κ'	0.04	0.11	0.19	0.27	0.34	5.51	11.06	16.61	22.06	27.67	4.14	8.28	12.46	16.62	20.76

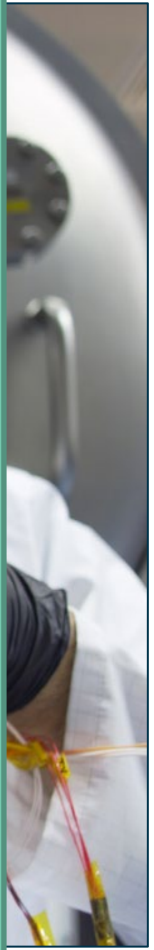

J. Nalepa et al.: Tow
2021, 13(8), 1532 (h

Estimating soil moisture from HSI: data acquisition

https://platform.ai4eo.eu/seeing-beyond-the-visible

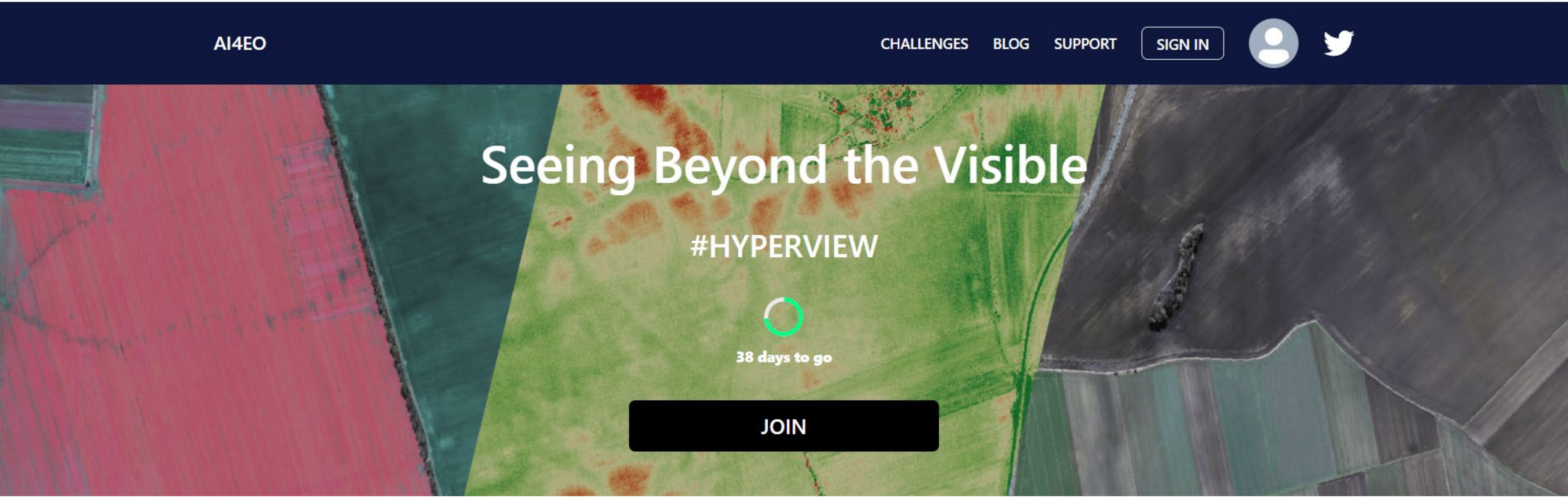

Estimating soil moisture from HSI: data acquisition

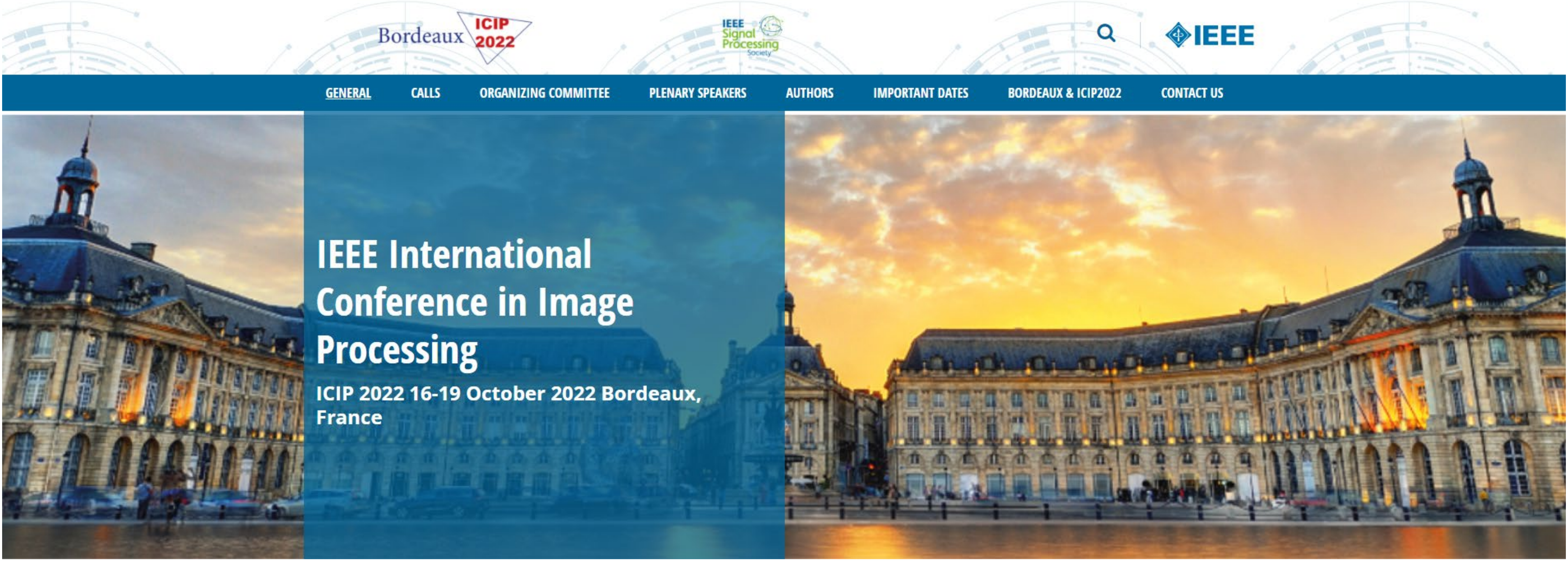

Super-resolution of Sentinel-2 temporal image stacks

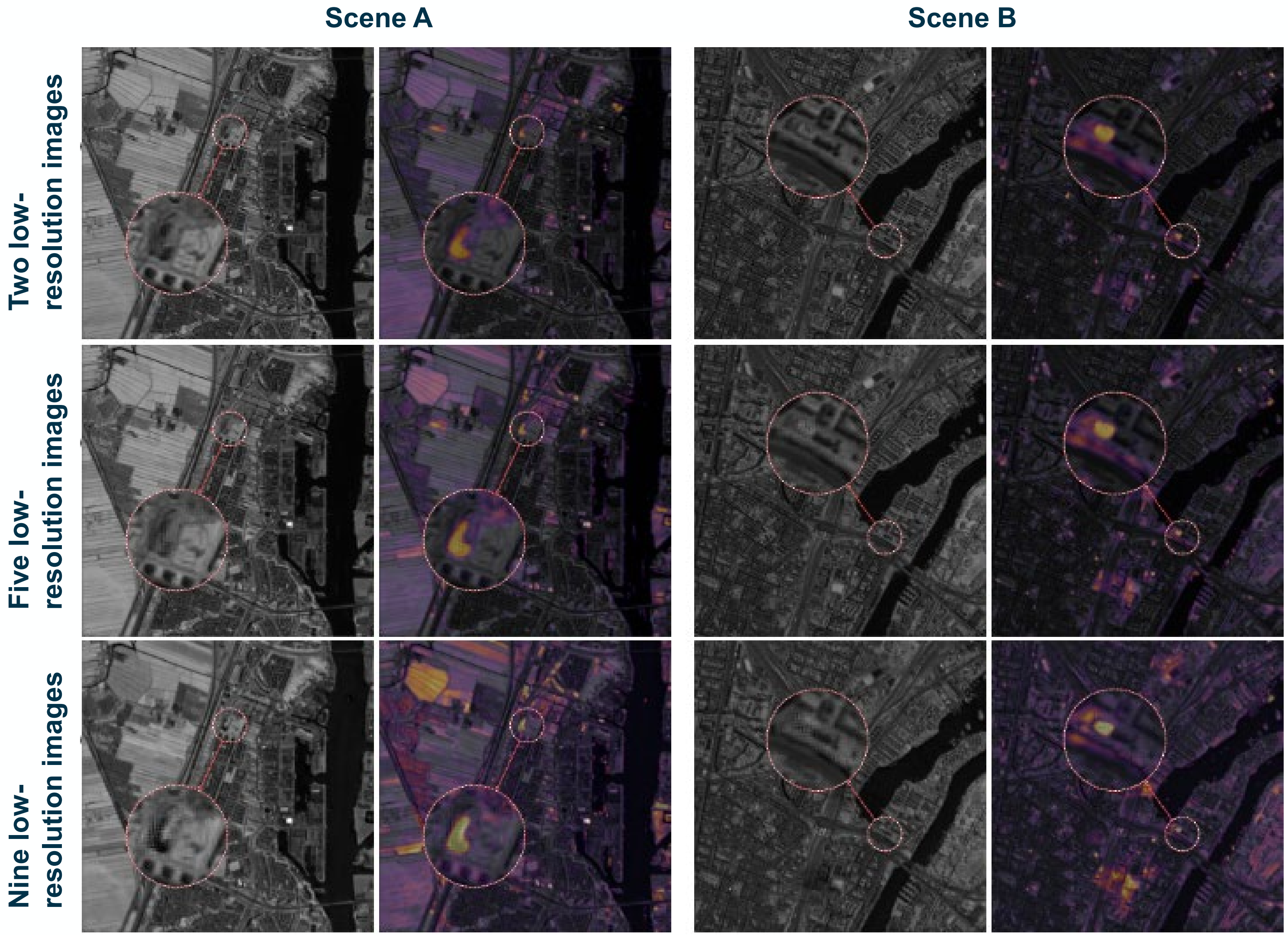

Super-resolution satellite images – mean opinion score

8. In which of the following images it is the MOST CHALLENGING to distinguish separate trees? *

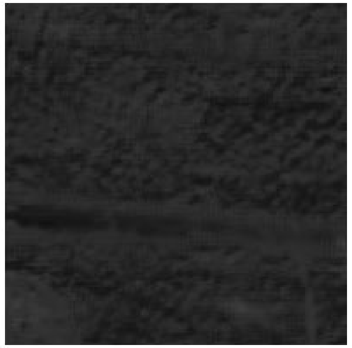

Image 1

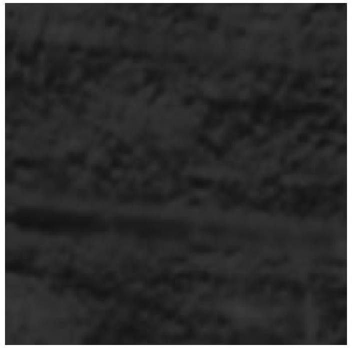

Image 2

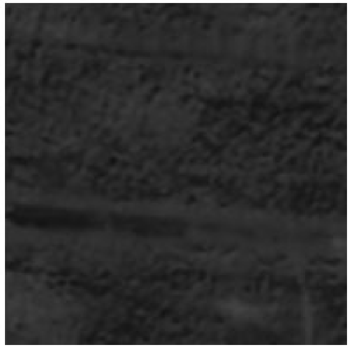

Image 3

10. Which of the following images presents the coastal area in the LEAST ACCURATE (LEAST DETAILED) way? The area of interest is rendered in red in the reference image. *

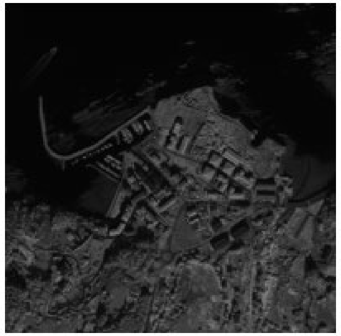

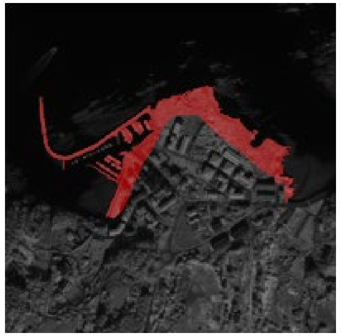

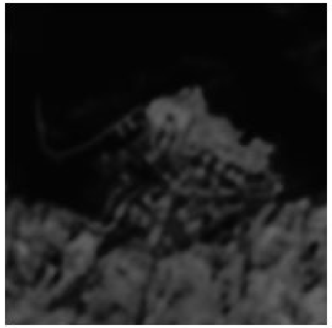

Image 1

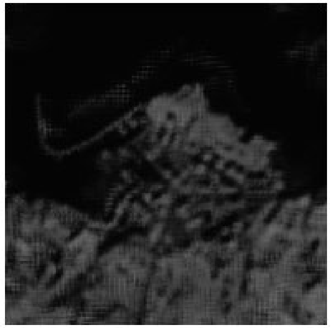

Image 2

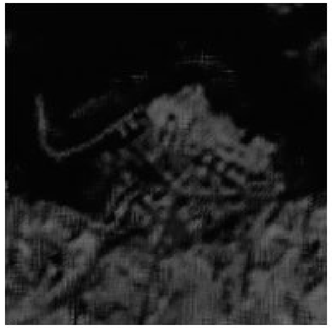

Image 3

Benchmarking anomaly detection from telemetry data

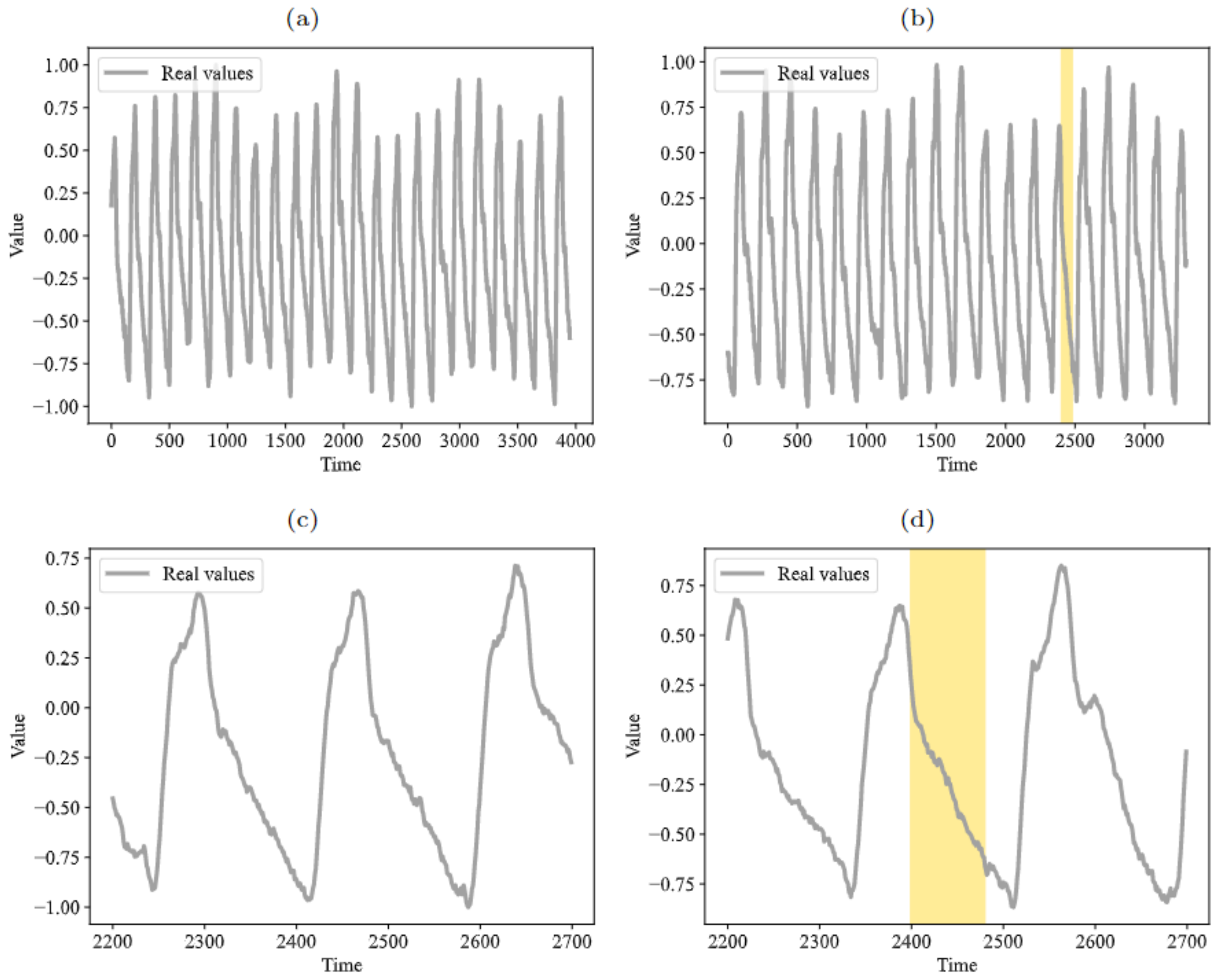

Examples of the (a) training and (b) test parts of the sequences available in the Hexagon-ML benchmark dataset, together with the zoomed parts of the (c) training and (d) test sequence. In each test part, there is always one anomalous event—the ground-truth anomaly is annotated in yellow. In gray, we present the real values of the signal.

Keogh, E., Dutta Roy, T., Naik, U. & Agrawal, A (2021). Multi-dataset Time-Series Anomaly Detection Competition, SIGKDD 2021. https://compete.hexagon-ml.com/practice/competition/39/

Benchmarking anomaly detection from telemetry data

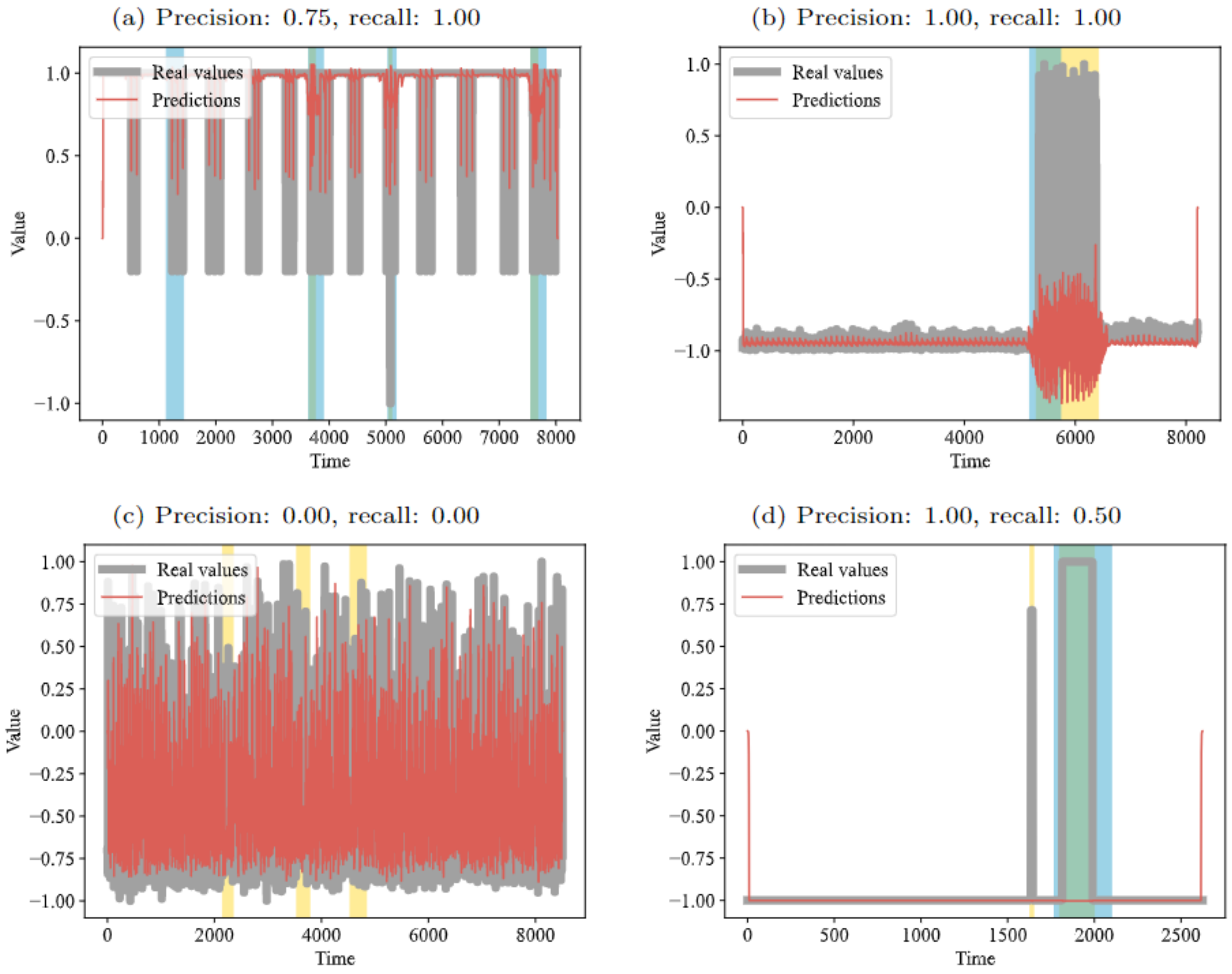

Examples of the precision and recall values obtained for various-quality detections over the synthetic data which can contain more than one anomalous even. The ground-truth events are rendered in yellow, whereas the automated detections are in blue—if those overlap, the intersection is presented in green.

Keogh, E., Dutta Roy, T., Naik, U. & Agrawal, A (2021). Multi-dataset Time-Series Anomaly Detection Competition, SIGKDD 2021. https://compete.hexagon-ml.com/practice/competition/39/

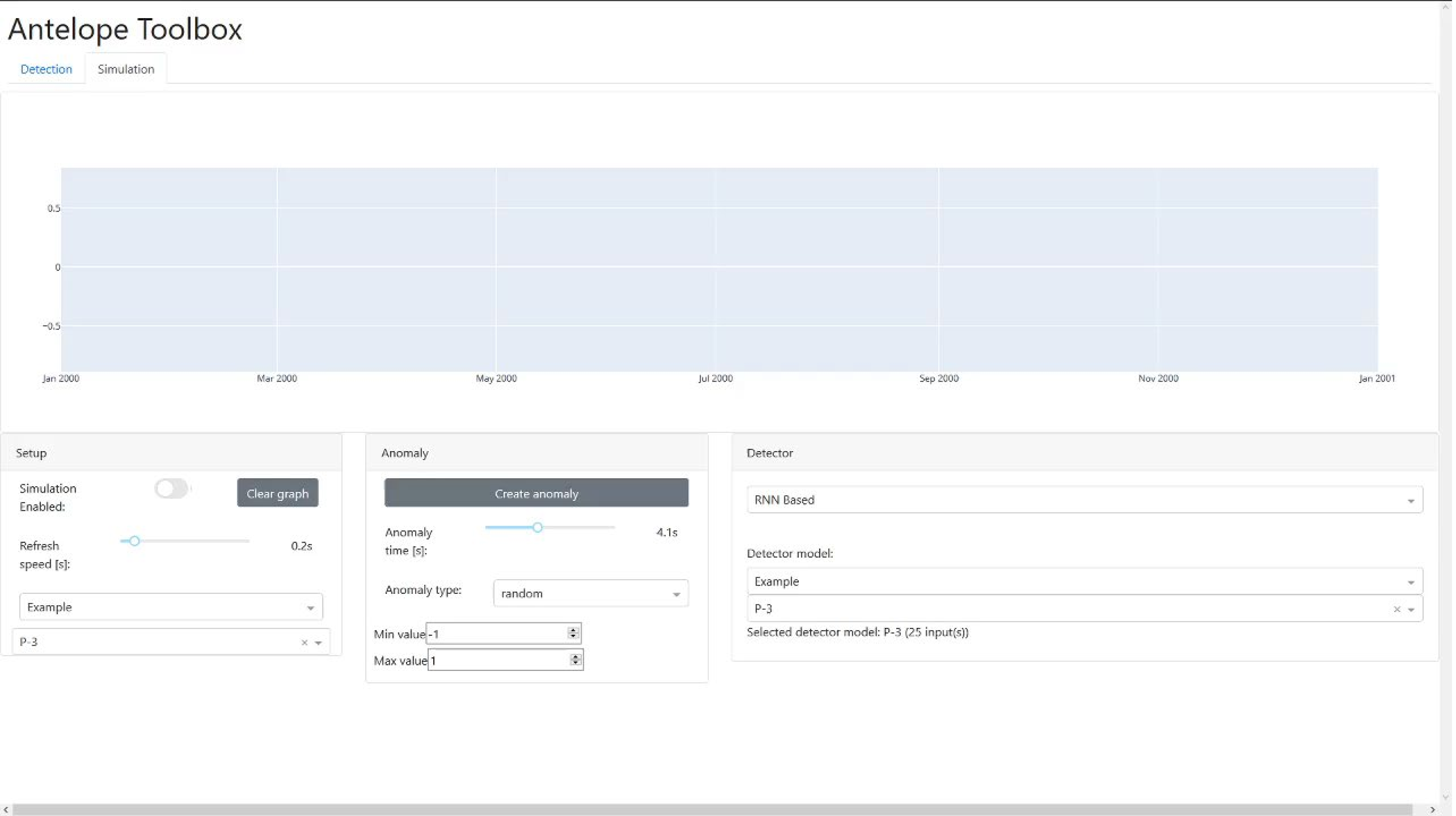
Antelope Toolbox
Detection
Simulation
0.5
0
−0.5
Jan 2000
Mar 2000
May 2000
Jul 2000
Sep 2000
Nov 2000
Jan 2001
Setup
Simulation Enabled:
Clear graph
Refresh speed [s]:
0.2s
Example
P-3
Anomaly
Create anomaly
Anomaly time [s]:
4.1s
Anomaly type:
random
Min value -1
Max value 1
Detector
RNN Based
Detector model:
Example
P-3
Selected detector model: P-3 (25 input(s))

What happens with real-life data?

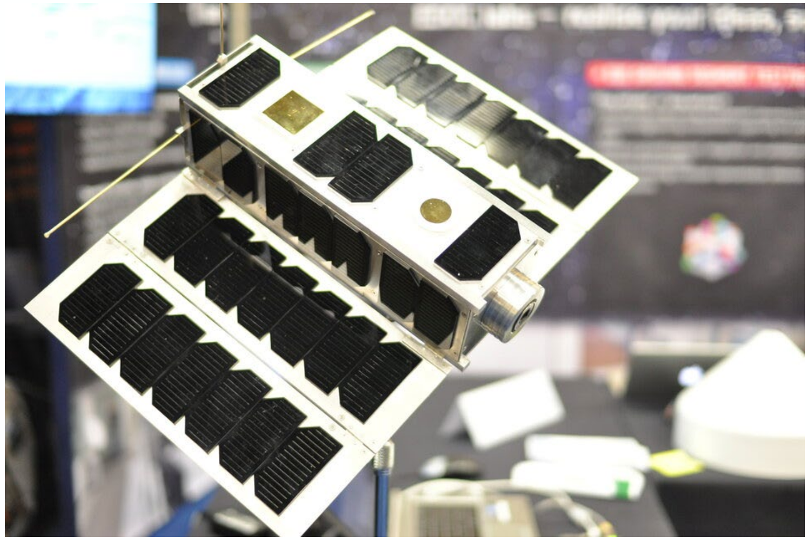

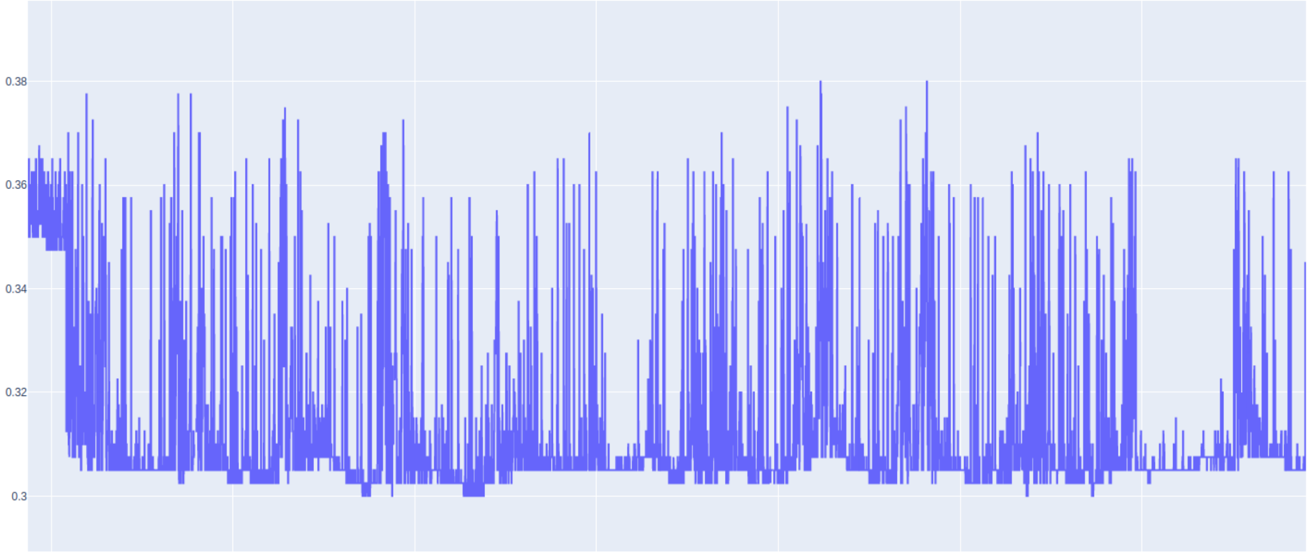

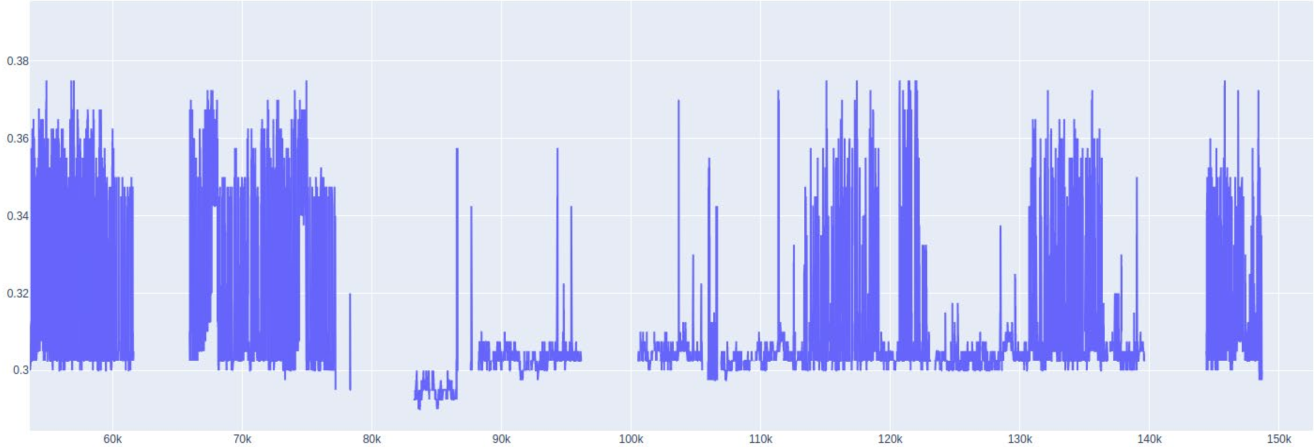

Values of SEP8260p: continuous fragment above, gaps visible below living planet symposium | BONN 23–27 May 2022

TAKING THE PULSE OF OUR PLANET FROM SPACE

Toward fair validation of AI algorithms for (not only) EO

Jakub Nalepa | jnalepa@ieee.org | KP Labs/Silesian University of Technology

KP LABS

May 27, 2022


OPEN
3dB